Journal of Power Sources 247 (2014) 1–8

Contents lists available at ScienceDirect

Journal of Power Sources

journal homepage: www.elsevier.com/locate/jpowsour

A comparative study of different binders and their effects on electrochemical properties of $LiMn_2O_4$ cathode in lithium ion batteries

Zhian Zhang [a,b], Tao Zeng [a], Yanqing Lai [a,b], Ming Jia [a,b], Jie Li [a,b,*]

[a] School of Metallurgical Science and Engineering, Central South University, Changsha 410083, China
[b] Engineering Research Center of High Performance Battery Materials and Devices, Research Institute of Central South University in Shenzhen, Shenzhen 518057, China

HIGHLIGHTS

- Physical properties of the pristine PVDF, CMC and PAA binders are researched.
- Electrodes with four binder systems are fabricated to compare physical properties.
- Rates performances and 25 & 55 °C cycle performances of the four cathodes are tested.
- The $LiMn_2O_4$ cathode with PAA/NMP binder system shows improved cycle performances.

ARTICLE INFO

Article history:
Received 26 March 2013
Received in revised form
17 July 2013
Accepted 14 August 2013
Available online 27 August 2013

Keywords:
$LiMn_2O_4$ cathode
Binder
Properties comparisons
Polyacrylic acid

ABSTRACT

Physical and chemical properties of poly(vinylidene fluoride) (PVDF), sodium carboxymethyl cellulose (CMC) and polyacrylic acid (PAA) binders are investigated in this paper, including functional group analysis, crystallinity and thermal properties. Then $LiMn_2O_4$ cathodes with four different binder systems (PAA binders/NMP solvent, PVDF binders/NMP solvent, PAA binders/H_2O solvent and CMC binders/H_2O solvent) are prepared, and their adhesion strengths, swelling properties, morphologies and electrochemical properties are studied. The results show that the $LiMn_2O_4$ cathode with PAA/NMP system displays the best cycle performances at both 25 °C and 55 °C among these four cathodes; the better capacity retention for $LiMn_2O_4$ cathode with PAA/NMP system is related to strong binding ability, appropriate swelling property and homogeneous distribution of particles inner the electrode.

1. Introduction

In the past few decades, lithium ion batteries have attracted considerable attention due to their promising applications in electric vehicles, hybrid electric vehicles and smart grids [1–3]. Intense worldwide efforts are under way to develop batteries with excellent performances to meet the ever-increasing demand for people's daily life. Traditionally, most researches were focused on the active material optimizations to enhance the electrochemical properties of lithium ion batteries [4–6], while less attention was devoted to the advancement of the electrically inactive components of battery electrodes, such as binders. Yet in recent years, many studies have shown that many important battery characteristics, such as the stability and rate performances, are critically dependent on the binder's properties [7–10].

Binder is an important part of electrode formulation because it can maintain the physical structure of the electrode; without a binder, the electrode would fall apart. A perfect binder should have high adhesion ability for the electrode materials to the current collector, as well as the ability to form a good electric network between the active material and conductive carbon, to facilitate electron transport and lithium ion diffusion [11].

Traditional poly(vinylidene difluoride) (PVDF) is the most widely used binder in commercial lithium ion batteries as it exhibits excellent electrochemical stability and bonding strength. However, it has been know that at elevated temperatures, the fluorine contained PVDF might react with lithiated graphite (Li_xC_6) and metal lithium via an exothermic reaction to form more stable LiF and unsaturated >C=CF– bonds, thus leading to a risk of

* Corresponding author. School of Metallurgical Science and Engineering, Central South University, Changsha 410083, China.
E-mail address: csulijie@126.com (J. Li).

0378-7753/$ – see front matter © 2013 Elsevier B.V. All rights reserved.
http://dx.doi.org/10.1016/j.jpowsour.2013.08.051

thermal runaway [12]. In addition, as mentioned by Zhang et al. [13], PVDF is readily swollen, gelled or dissolved by nonaqueous liquid electrolytes to form viscous fluid or gel polymer electrolyte, which results in desquamation of electrode particles hence capacity-fading and cycle life shortening. Moreover, the low flexibility of PVDF cannot meet the demands of long cycle life for cathode due to breaking of the bonds between the active material and the conductive carbon when the durable expansion/contraction process of the active material occurs during cycling [14].

Another kind of binder that is commonly used in commercial lithium ion batteries is the sodium salt of carboxymethyl cellulose (CMC). The greatest advantage of CMC is that it allows processing of electrode slurries with water solvent rather than with polluting, environmentally unfriendly, volatile organic compound-based solvents. Moreover, this kind of water-soluble binder is cheap and easy to dispose at the end of the battery life, thus definitely leading to cheaper and greener electrode processing [15]. Due to its apparent advantages, the applications of CMC as the binders in lithium ion batteries have been reported frequently [9,16]. However, the CMC binder is usually used together with styrene–butadiene rubber (SBR), another kind of binder to get a better performance.

Recently, some new species of binders have been employed in lithium ion batteries [7,17–19]. Among them, polyacrylic acid (PAA) has received large attention. The chemical structure of PAA is shown in Fig. 1, along with that of PVDF and CMC for comparison. PAA can dissolve in both water and *N*-methyl-2-pyrrolidone (NMP), and it can form strong hydrogen bonds with both active materials and current collectors due to carboxylic acid functional groups. PAA as a binder for Sn, Si alloys [20–26], natural graphite anodes [27–31], and $LiFePO_4$ cathodes [19,32–34] had previously been reported. In our previous works [33,34], $LiFePO_4$ cathode with PAA as binder and NMP as solvent was prepared, both the room temperature [33] and elevated temperature electrochemical performances [34] had gotten better results than that of the conventional $LiFePO_4$ cathodes with PVDF binder.

Similarly to $LiFePO_4$ material, $LiMn_2O_4$ as one of the most promising large-scale commercial cathodes for lithium ion batteries has shown its overwhelming advantages of low cost and environmental friendly. However, we know that the $LiMn_2O_4$ suffers fast capacity fading during cycling, especially at elevated temperatures due to Jahn–Teller distortion and Mn^{3+} ions dissolution into the electrolyte [35,36]. Many efforts were taken to improve electrochemical performances of $LiMn_2O_4$, including $LiMn_2O_4$ materials optimizing and electrolyte improvement. Here we conducted experiments to investigate whether or not the binders can improve the electrochemical performances of $LiMn_2O_4$ cathode, especially the PAA binder, which can improve the performances of $LiFePO_4$ cathode and other anodes. To the best of our knowledge, there is no report about the application of PAA as a binder for $LiMn_2O_4$ cathode.

In this work, we studied the effects of PVDF, CMC and PAA binders on the electrochemical properties of $LiMn_2O_4$ cathodes. At first, physical and chemical properties of the pristine binders have been researched, and then $LiMn_2O_4$ cathodes with different binders have been prepared to test the electrochemical performances and some physical properties. Herein we have made a research of four different cases: $LiMn_2O_4$ cathodes with PAA binders and NMP solvent (PAA/NMP), PVDF binders and NMP solvent, PAA binders and H_2O solvent (PAA/H_2O), CMC binders and H_2O solvent.

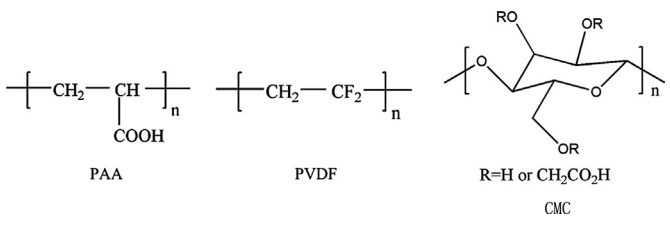

Fig. 1. Chemical structures of PAA, PVDF and CMC.

2. Experiment

The commercial $LiMn_2O_4$ powders were provided by Tianjin Lishen Battery Co., Ltd., China with detailed specifications as follows: Li mass percent (4.0%), average particle size D_{50} (15 μm), tap density (2.1 g cm^{-3}) and BET specific surface area (0.6 m^2 g^{-1}). Super P with an average particle size of 40 nm was acquired from TIMCAL Graphite & Carbon, Switzerland. PAA powder (M_w = 450,000) was purchased from Sigma–Aldrich. PVDF (HSV900, M_w = 1,000,000) was supplied by Arkema, France. The type 2200 sodium carboxymethyl cellulose (CMC) was come from DAICEL, Japan.

The three kinds of binder powders were characterized by scanning electron microscopy (SEM, Quanta-200, FEI), X-ray diffraction (XRD, Rigaku D/max), Fourier transform infrared spectroscopy (FTIR, Nicolet 6700) and solubility tests. Additionally, these three binder powders were extruded by a hydraulic press to form a cylinder with diameter of 10 mm for thermal diffusivity and thermal expansion rate tests. The thermal expansion rates were tested using electronic dilatometer (DIL 402PC netzsch), sample mass for the test was 1 g, and rate of temperature-increase was 5 K min^{-1} from 25 °C to 80 °C. The whole process was finished in the N_2 atmosphere, with the N_2 flow rate 100 mL min^{-1}. For the thermal diffusivity date, it was tested by using thermophysical property measuring apparatus, sample mass for the test was 1 g, and the temperature was 25 °C.

For electrode preparation, measured amounts of $LiMn_2O_4$, Super P and binder (80:10:10 by mass) were added into a container with suitable amounts of solvent (NMP for PAA, PVDF, deionized water for PAA, CMC, respectively). Details on the electrodes preparation, cells configuration and electrochemical performances tests had been described clearly in our previous works [33,34].

Adhesion strength of the $LiMn_2O_4$ composite layers onto the Al current collectors were tested using 180° peel tester (XLW PC, Labthink) with the rate of 30 cm min^{-1}. Swelling properties of the binders were examined from weight gain of the electrodes after soaking them in the electrolyte for 48 h. Morphologies of the electrodes were conducted by SEM (Quanta-200, FEI).

3. Results and discussion

3.1. Physical and chemical properties of the pristine binders

Fig. 2 shows the FTIR spectra of the PAA, PVDF and CMC binders. For PAA binder, the main absorbance band at 1720 cm^{-1} is assigned into the free carboxylic acid group (–COOH), also we can find two absorbance bands at 1640 and 1450 cm^{-1}, which are from the associated two carboxylic groups, forming hydrogen bonding to crosslink the PAA chains [22,37]. For CMC binder, the peaks of sodium carboxylate group ($-COO^-Na^+$) at 1600 and 1420 cm^{-1} can be found clearly, vibrational bands between 900 and 1100 cm^{-1} are attributed to the ether groups (C–O–C) from cellulose [10]. For PVDF binder, the vibrational bands at 1180 and 880 cm^{-1} are ascribed to the stretching frequencies of CF_2. Additionally, the bands at 973, 879, 840, 762, 612 cm^{-1} are crystallization peaks which are assigned to the vibration of the crystallization PVDF

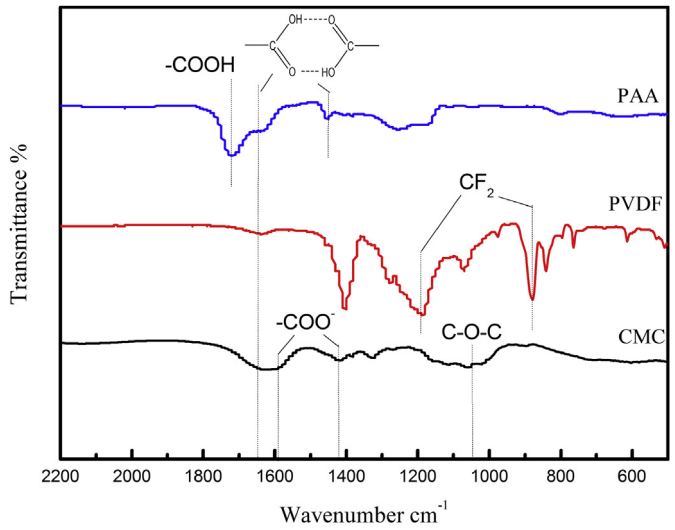

Fig. 2. FTIR spectra of PAA, PVDF and CMC.

according to Peng's report [38]. That is to say PVDF is a semicrystalline polymer, which will be further discussed in the later section.

Such differences in molecular structures can highly influence the binding abilities of different binders. According to Cai's reports [32], due to the existences of carboxylic groups in PAA and CMC binder, ester-like chemical bonds between the polymer molecules and the hydroxyl groups on the surfaces of active material powders can be formed, thus leading to strong binding ability in the composite electrodes. Additionally, for PAA binder, the formed hydrogen bonds between the associated two carboxylic groups (1640 and 1450 cm^{-1}) can crosslink or bridge the PAA chains and bring more excellent binding ability than CMC according to the other's researches [22,37]. In the case of PVDF, the bonding ability comes from the formation of very weak hydrogen bonds with F atoms and active materials [8], which result in relatively weak adhesion as displayed in the later section.

The crystallinities of the binders were examined by XRD. Fig. 3a presents X-ray diffraction patterns of the three binders, since the diffraction peak around 2θ = ca. 20° for PVDF is sharper than the other two polymers. Note that the PVDF has a better crystallinity than PAA and CMC because it is a semicrystalline polymer with a polymorphism according to Han's report [39]. The results of XRD are similar with the FTIR in Fig. 2. Also, the conclusions can be confirmed by the SEM images of the three binder pristine solid powders as show in Fig. 3b–d. We can see from Fig. 3b that PVDF is composed of small spherical particles, gather together like roe. The result suggests that PVDF has regular shape, which is one of the features of crystal. While for PAA and CMC binders, only irregular shape particles can be observed in Fig. 3c and d, which indicates that PAA and CMC are amorphous substances.

The differences in the crystallinity may highly influences the morphologies of polymer films, which are formed after dissolving the binders in solvent and then drying [21–23,40]. The PVDF is a semicrystalline polymer, so that its main chains are in part bundled together to form the crystallite region during drying. Therefore, the amount of the polymer, which is effectively used to bind the electrode materials is reduced [23]. Consequently, the PVDF polymer

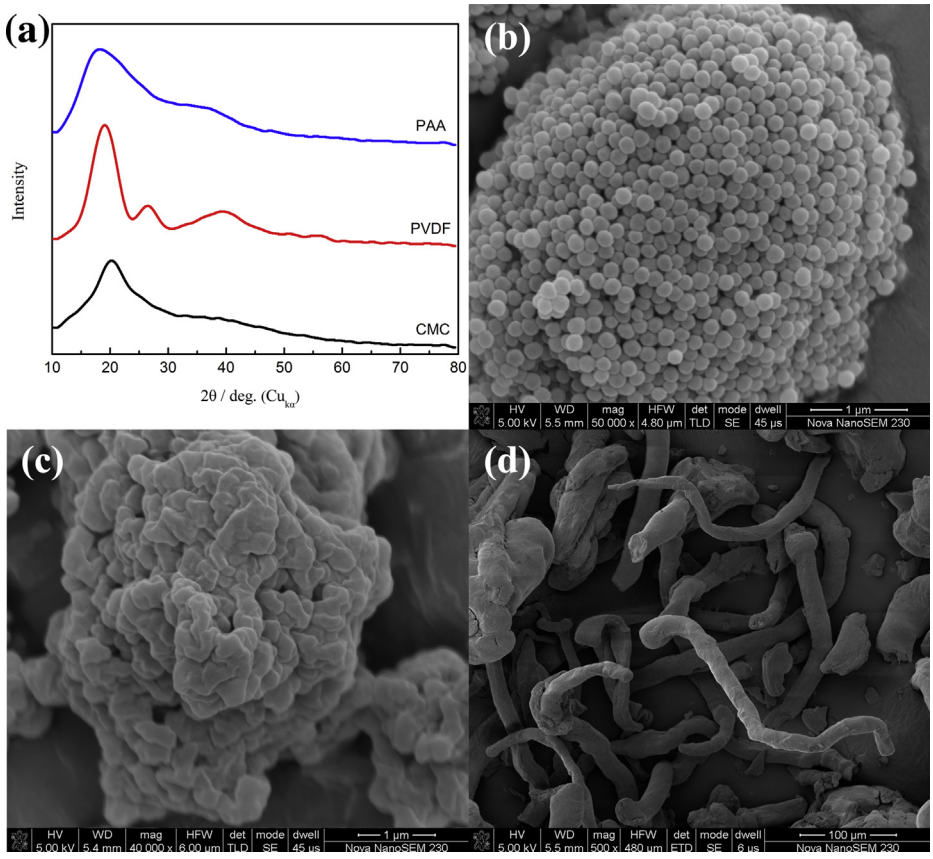

Fig. 3. (a) for X-ray diffraction patterns of the three binders, (b), (c) and (d) for SEM of PVDF, PAA and CMC pristine solid powders, respectively.

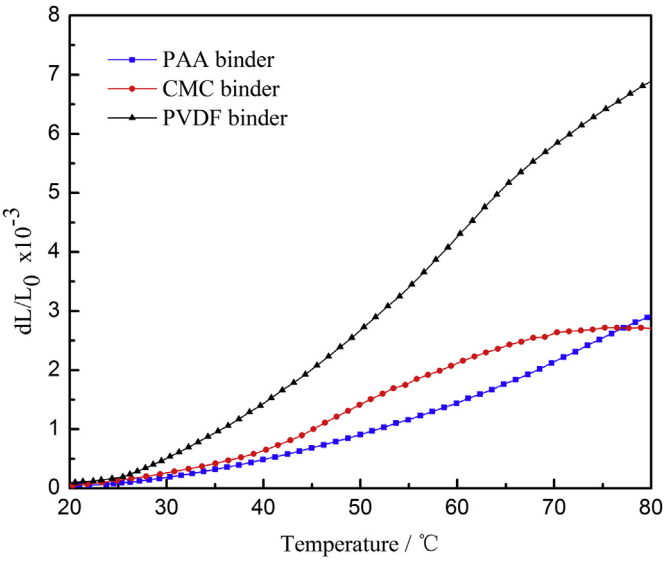

Fig. 4. Thermal expansion rate curves of PAA, PVDF and CMC binders at the temperature rang from 20 °C to 75 °C.

film possesses many pores [40], whereas the amorphous PAA film is a uniform, dense, and transparent one, like glue.

For this reason, $LiMn_2O_4$ electrodes prepared using PVDF and PAA binders will show apparently differences in morphology. The glue-like PAA binder can cover the $LiMn_2O_4$ active materials completely and uniformly, like a protective film, thus improving the electrochemical performances of electrodes due to the decrease of electrolyte decomposition [27–29] or other reasons [34]. However, for PVDF, it covers the $LiMn_2O_4$ active materials like a net with many pores [40], so that the electrolyte can contact the active materials directly, leading to electrochemical performances deterioration.

Thermal properties concerning thermal diffusivity and thermal expansion rate of the polymers were tested. Fig. 4 shows the thermal expansion rate curves of the three binders between 20 °C and 80 °C, the normal using temperature range of lithium ion batteries. We can see that the PVDF binder has larger thermal expansion rate dL/L_0 (L for the length of the sample at some temperature, L_0 for the original length of the sample) than CMC and PAA binders. This is because thermal expansion generally influenced by intermolecular forces, the intermolecular force of PVDF polymer (mainly van der Waals force) is weaker than that of PAA and CMC polymers, which not only the van der Waals force, but also hydrogen bonds exist between the molecular [22,37]. The result indicates that when the temperature increases, the PVDF binder has the largest volume expansion, and the inner pressure of the battery made with PVDF binder is largest, which tends to trigger safety problems.

Thermal diffusivity of the polymers were illustrated in Table 1, the PAA binder has the largest thermal diffusivity for 3.1×10^{-3} cm^2 s^{-1}, which is about three times larger than that of CMC binder (1.0×10^{-3} cm^2 s^{-1}) and PVDF binder (9.1×10^{-4} cm^2 s^{-1}). The difference in the thermal diffusivity will have an impact on the safety performance of batteries. Particularly, when there is a momentary high temperature emerges in the battery, the PAA binder with the larger thermal diffusivity can spread the heat to the outside more quickly. The temperature sensor outside the battery can respond timely. Thus, the occurrence of safe problem decreases.

Table 1
Thermal diffusivity of the three polymers.

Binder	Thermal diffusivity cm^2 s^{-1}
PVDF binder	9.1×10^{-4}
PAA binder	3.1×10^{-3}
CMC binder	1.0×10^{-3}

3.2. Physical properties of the electrodes with four binder systems

Fig. 5 shows the SEM images of $LiMn_2O_4$ electrodes using four different binder systems. In Fig. 5a and b, we can see that both the cathodes made with PVDF and PAA/NMP binder systems have good dispersities. While big aggregate particles can be found in the PAA/H_2O binder system electrode (Fig. 5c). Additionally, the CMC binder electrode shows a big difference from the others, some $LiMn_2O_4$ particles are exposed on the electrode surface. Such morphology distinctions are determined by the different physicochemical properties of three binders. Comparing the SEM images of the two PAA binder electrodes (Fig. 5b and c), we can find that the electrode dispersities are largely changed by using different solvents. According to Lestriez's report [41], we propose that the main reason is the difference of viscosity between the two binder solutions, which are formed after dissolving the binders into the solvents. The differences of the electrode dispersity may influence electrochemical performances of the four cathodes, which will be represented later in the cycle performance discussion.

Adhesion strengths of the composite electrodes were evaluated by 180° peel test. Table 2 summarizes the adhesive strengths to the aluminum current collectors for the $LiMn_2O_4$ composite electrodes with the four different binder systems. The load to peel the PVDF composite from current collector was measured to be 0.32 N cm^{-1}, which is considerably smaller than 1.5 N cm^{-1} observed for the PAA/H_2O and CMC binder system $LiMn_2O_4$ composites, and the adhesion strength of PAA/NMP composite is 10 times larger than that of PVDF, for 3.2 N cm^{-1}. The mechanical strength of the composite layer is improved by the application of PAA binder and NMP solvent. For the two PAA binder electrodes with NMP and H_2O, due to some aggregation existing inner the PAA/H_2O binder electrode (Fig. 5c), thus leading to uneven distribution of binder. Adhesion strength of the PAA/H_2O binder electrode may be weaker than the uniformly distributed PAA/NMP binder electrode (Fig. 5b).

A binder's high adhesive strength plays an important role in improving the electrode performances especially the cycle ability. The cathode with PVDF binder easily loses the electrical contact with the current collector compared with the cathode using PAA/NMP binder system, which can sticks the particles on the Al substrate to withstand the excessive penetration of electrolyte solution and the volume change of the electrode during cycling. After the cycling test, the PVDF composite electrode can be detached from the aluminum current collector easily, while the other three electrode composites tightly stuck to the current collectors, as can be seen in Fig. 6. Such an adhesive strength result can be an important reason why $LiMn_2O_4$ with PAA/NMP shows better cycle ability than PVDF binder cathode as will be represented later.

Swelling properties of the electrode films were examined by soaking them in the electrolyte solution (1 mol L^{-1} $LiPFe_6$ dissolved in EC/DMC/EMC 1:1:1 by mass) at room temperature for 48 h. Then the electrodes were taken out to weigh the m_1 after removing the electrolyte on the surface with the filter papers. Here we define the initial weight of the electrodes as m_0. The increased mass percent of the polymer films $(m_1 - m_0)/m_0$ were summarized in Table 2. In this experimental condition, weight gain of the polymer film by the absorption of the carbonate solution is 20.8%, 5.2%, 10.3% and 8.3% of the initial weight for PVDF, PAA/NMP, PAA/H_2O and CMC binder system, respectively. For the two kinds of PAA binder electrodes,

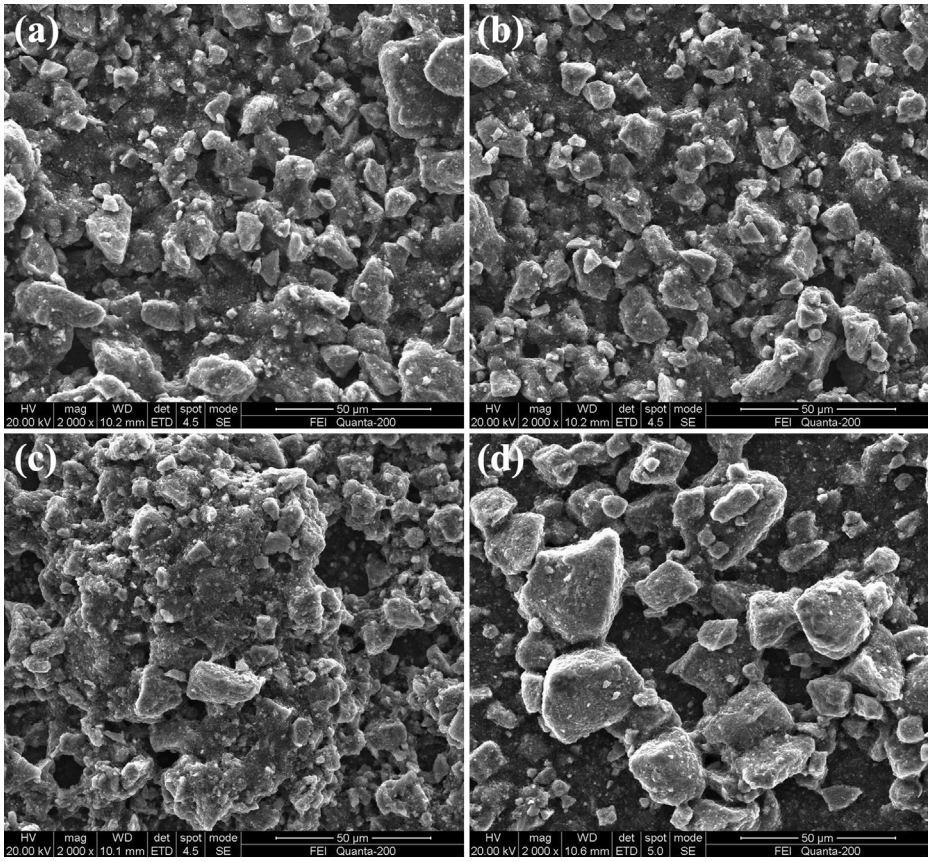

Fig. 5. SEM images of $LiMn_2O_4$ electrodes made with the four binder systems, (a) for the cathodes made with PVDF, (b) for PAA/NMP, (c) for PAA/H_2O and (d) for CMC binder system, respectively.

due to lots of aggregation particles existing in the PAA/H_2O binder electrode, interspaces between the aggregation big particles are larger than that of PAA/NMP binder electrode. So the PAA/H_2O binder electrode may absorb more liquid when soaking it in the electrolyte.

Another experiment of the swelling character is added by soaking the binders in the electrolyte solution directly. And Fig. 7 records the beginning and end situation (after 48 h). PVDF powders easily swells, forming a viscous, gel-like fluid product, which is in accordance with other reports [13,23]. In contrast, PAA and CMC do not swell at the same experimental condition. Reasons of the phenomenon described above have not been found out by us yet.

The swelling of binders must be also the important factors for reversible cycling. PVDF can be swelled by absorbing electrolyte, leading to the penetration of electrolyte solution into the whole composite electrode and desquamation of electrode particles. The electrical conductive network in the PVDF composite electrode might be in part loosened or broken by the inordinate penetration of the electrolyte according to Komaba's report [22], resulting in capacity-fading and cycle life shortening after long time cycling. While for PAA binder composite electrode, the polymer can effectively prevent the excessively penetration of the electrolyte and improve the cycle performance compare to PVDF system.

Table 2
Adhesion strengths and swelling properties of the $LiMn_2O_4$ cathodes with four binder systems.

Electrode	Adhesion strength N cm^{-1}	Swelling property %
$LiMn_2O_4$/PVDF	0.32	20.8
$LiMn_2O_4$/PAA/NMP	3.26	5.2
$LiMn_2O_4$/PAA/H_2O	1.57	8.3
$LiMn_2O_4$/CMC	1.50	10.3

3.3. Electrochemical performances

The C-rate performances of the $LiMn_2O_4$ electrodes with different binder systems were tested at 25 °C, as shown in Fig. 8. Among all of the binder systems, CMC exhibits the largest discharge capacity at 0.1 C rate (137.7 mAh g^{-1}). The cathode made with PAA/NMP binder system ranks second, with a capacity of 131.3 mAh g^{-1}. The remaining two systems have the same discharge capacity for about 124 mAh g^{-1}. However, the results are different at 3 C rate, at which the discharge capacity of PVDF binder is the largest. And the capacity retention at higher rates is 74.9%, 66.2%, 66.2% and 63.6%, for PVDF, PAA/NMP, PAA/H_2O and CMC systems, respectively.

As mentioned above [23,29,40], the semicrystalline PVDF polymer possesses many pores, whereas the amorphous PAA is a uniform, dense, and transparent film, like glue. The glue-like PAA

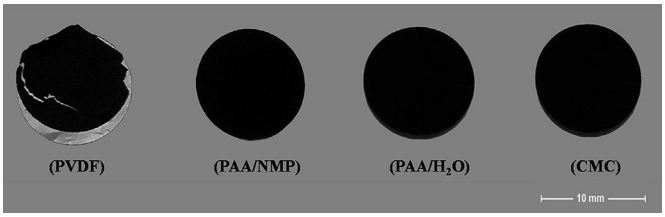

Fig. 6. Morphologies of the four electrodes, the electrodes were taken out from the batteries after 200 cycles.

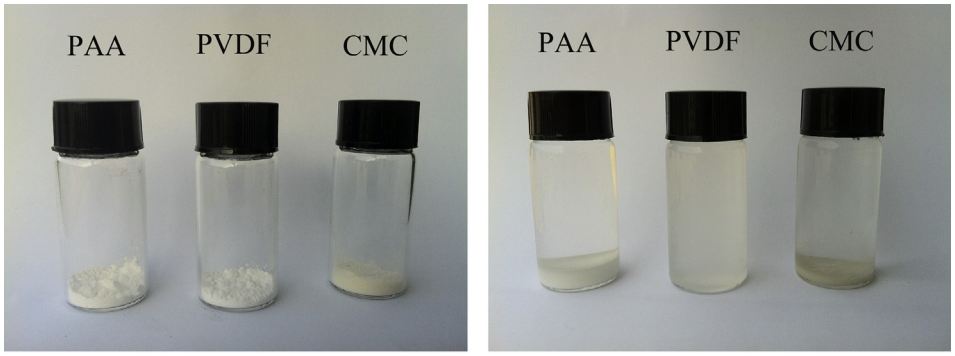

Fig. 7. The difference in the swelling of the polymer powders by addition of the electrolyte solution (1 mol L^{-1} in EC:DMC:EMC = 1:1:1 by mass).

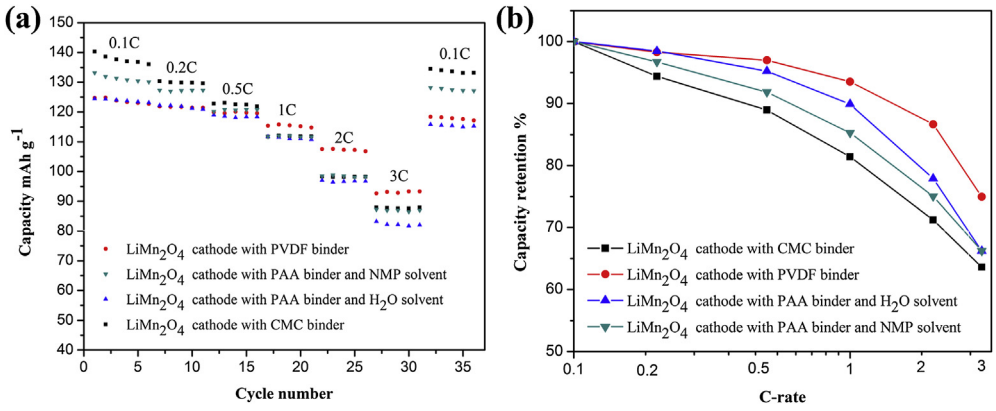

Fig. 8. (a) Rate performance of electrodes made with different binder systems; (b) discharge capacity retention at various current densities.

binder can cover the active materials completely and uniformly to decrease electrolyte decomposition, but at the same time, it may influence the speed of lithiation and delithiation, especially at a high rate situation, where the Li^+ get in and out the active materials at high speed. But the Li^+ can go through the pored PVDF binder easily. This is why the discharge capacity of PVDF binder cathode at higher rate is better than the PAA systems. For the CMC binder cathode, the poor capacity retention at higher rates may be related to the uneven distribution of particles and poor conductive network in the cathode as seen in the SEM in Fig. 5d.

The cyclic performances at 1 C of $LiMn_2O_4$ electrodes prepared with different binder systems are illustrated in Fig. 9. The order of capacity retention from best to worst is cathode with PAA/NMP, PVDF, CMC, PAA/H_2O binder system; they are 85.7%, 75.6%, 57.3% and 31.1% for 200 cycles, respectively. The cycling result of PVDF binder cathode is comparable to the report of others [4–6,36]. The better capacity retention of PAA/NMP binder system cathode can be related to the strong binding ability, appropriate swelling property as well as the homogeneous distribution of particles inner the electrode. And the cycle properties might be influenced by a small binding strength for PVDF binder electrode and imperfect dispersities for CMC and PAA/H_2O binder systems electrodes, respectively.

Fig. 10 shows the discharge curves of the four kinds of cathodes at various cycle numbers at 25 °C. All the 1st discharge curves of the four systems show lower voltage than the subsequent cycle. This is probably because of the incompletely immersing of electrodes by the electrolyte at the beginning of the cycle, some of the conducting matrix may not play role thus lead big impedance. The PVDF binder cathode has the best initial capacity (115 mAh g^{-1}), a slight higher than the other three systems (110 mAh g^{-1}). With the increasing of cycle number, the discharge voltage and capacity for the PAA/NMP binder system (Fig. 10a) almost remain the same, while the discharge voltage and capacity decline obviously for the other three binder systems, as shown in Fig. 10b, c and d. The result can be

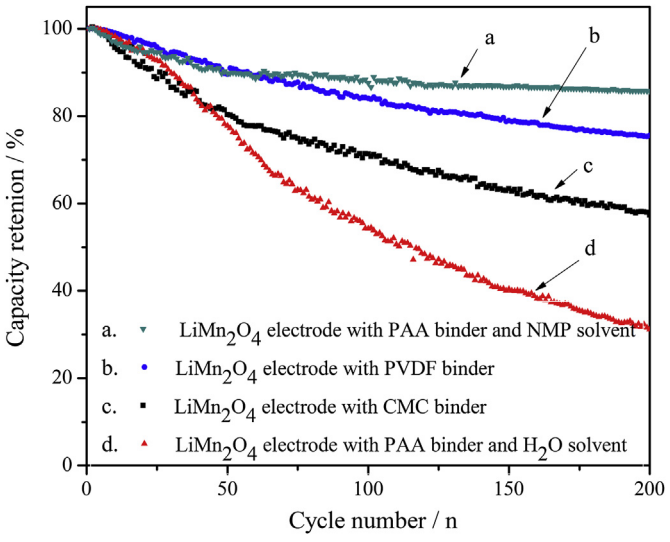

Fig. 9. Discharge cycle performances of $LiMn_2O_4$ cathodes with the four different binder systems at the rate of 1 C between 3 V and 4.3 V at 25 °C.

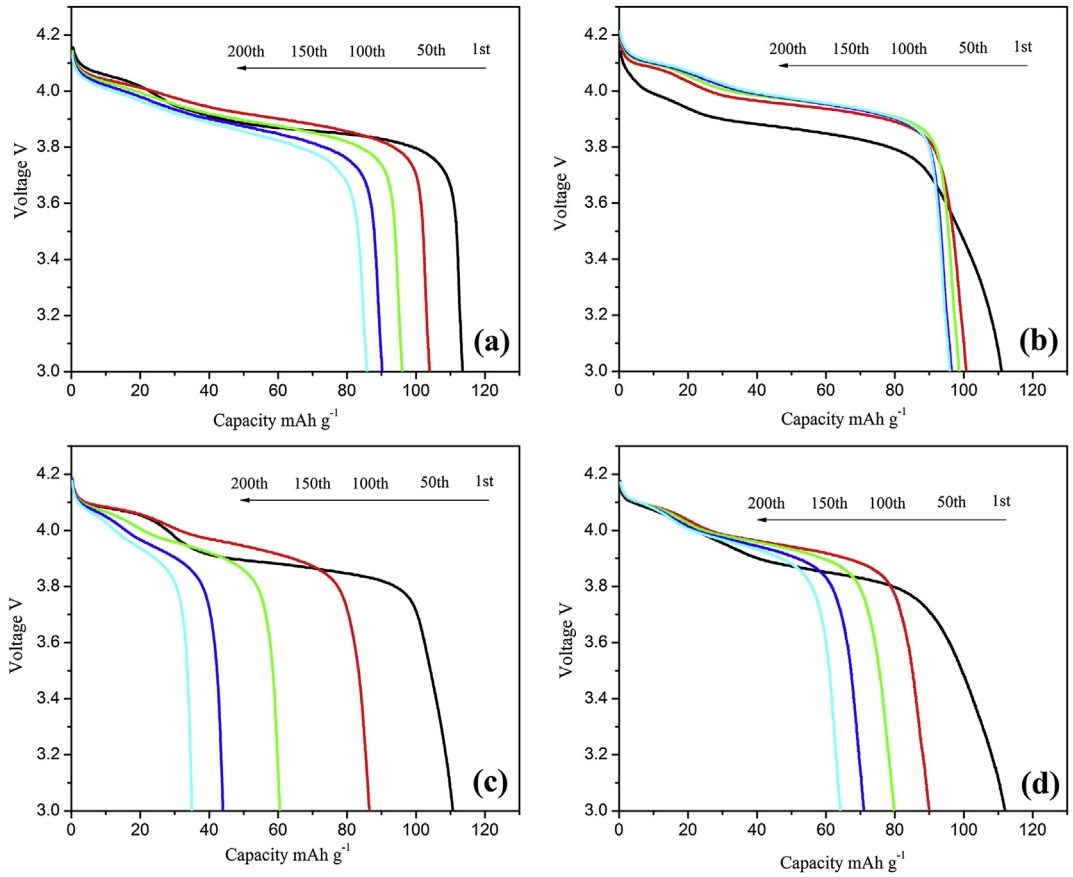

Fig. 10. 1 C discharge curves of the four kinds of cathodes at various cycle numbers at 25 °C, (a) for PVDF, (b) for PAA/NMP, (c) for PAA/H_2O and (d) for CMC binder system.

ascribed to the increasing potential polarization of the cathodes during the charge and discharge processes.

Fig. 11 presents cyclic performances of $LiMn_2O_4$ with the four binder systems at 55 °C at the rate of 0.5 C. The PAA/NMP binder system cathode generates the best capacity retention (74.8% for 100 cycles), the second largest retention is PAA/H_2O binder system for 72%, the third is PVDF for 67.6%, which is comparable to the report of Chen et al. [4–6], and the last one is CMC for 57.8%. Detail mechanisms for the PAA binder to improve the high temperature performances of $LiMn_2O_4$ cathode are being investigated by us, which will be discussed in further report.

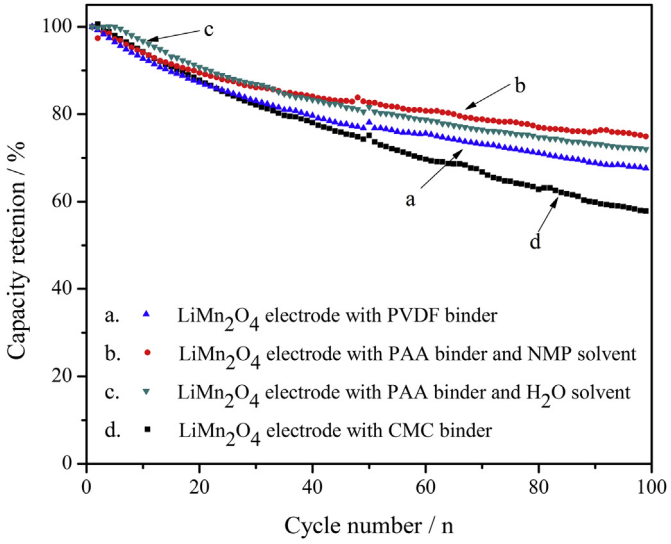

Fig. 11. Discharge cycle performances of $LiMn_2O_4$ cathodes with the four different binder systems at the rate of 0.5 C between 3 V and 4.3 V at 55 °C.

4. Conclusions

Electrochemical properties of $LiMn_2O_4$ cathode made with the four binder systems are studied in this report, and the cathode with PAA/NMP system shows the best cycle performances in both 25 °C and 55 °C among the four kinds of cathodes. The capacity retention is 85.7% for 200 cycles and 74.8% for 100 cycles, respectively. The better capacity retention of PAA/NMP binder system cathode can be related to the strong binding ability, appropriate swelling property as well as the homogeneous distribution of particles inner the electrode. The polymer binder has a great impact on the electrochemical performance of the electrodes, we believe that the research of binders will be a useful way for the development of lithium-ion battery technology in the future.

References

[1] B. Scrosati, J. Hassoun, Y.K. Sun, Energy Environ. Sci. 4 (2011) 3287–3295.
[2] M. Armand, J.M. Tarascon, Nature 451 (2008) 652–657.
[3] J.M. Tarascon, Phil. Trans. R. Soc. A 368 (2010) 3227–3241.
[4] Q. Chen, Y. Wang, T. Zhang, W. Yin, J. Yang, X. Wang, Electrochim. Acta 83 (2012) 65–72.
[5] L. Xiong, Y. Xu, T. Tao, J.B. Goodenough, J. Power Sources 199 (2012) 214–219.
[6] C. Qing, Y. Bai, J. Yang, W. Zhang, Electrochim. Acta 56 (2011) 6612–6618.
[7] I. Kovalenko, B. Zdyrko, A. Magasinski, B. Hertzberg, Z. Milicev, R. Burtovyy, I. Luzinov, G. Yushin, Science 334 (2011) 75–79.
[8] L. Gong, M.H.T. Nguyen, E.S. Oh, Electrochem. Commun. 29 (2013) 45–47.

[9] J. Xu, S.L. Chou, Q.F. Gu, H.K. Liu, S.X. Dou, J. Power Sources 225 (2013) 172–178.
[10] F.M. Courtel, S. Niketic, D. Duguay, Y.A. Lebdeh, I.J. Davidson, J. Power Sources 196 (2011) 2128–2134.
[11] H. Zheng, R. Yang, G. Liu, X. Song, V.S. Battaglia, J. Phys. Chem. C 116 (2012) 4875–4882.
[12] S.S. Zhang, K. Xu, T.R. Jow, J. Power Sources 138 (2004) 226–231.
[13] S.S. Zhang, T.R. Jow, J. Power Sources 109 (2002) 422–426.
[14] A. Guerfi, M. Kaneko, M. Petitclerc, M. Mori, K. Zaghib, J. Power Sources 163 (2007) 1047–1052.
[15] S.F. Lux, F. Schappacher, A. Balducci, S. Passerini, M. Winter, J. Electrochem. Soc. 157 (2010) A320–A325.
[16] J.P. Yen, C.M. Lee, T.L. Wu, H.C. Wu, C.Y. Su, N.L. Wu, J.L. Hong, ECS Electrochem. Lett. 1 (2012) A80–A82.
[17] H.K. Park, B.S. Kong, E.S. Oh, Electrochem. Commun. 13 (2011) 1051–1053.
[18] G. Liu, S. Xun, N. Vukmirovic, X. Song, P.O. Velasco, H. Zheng, V.S. Battaglia, L. Wang, W. Yang, Adv. Mater. 23 (2011) 4679–4683.
[19] J. Chong, S. Xun, H. Zheng, X. Song, G. Liu, P. Ridgway, J.Q. Wang, V.S. Battaglia, J. Power Sources 196 (2011) 7707–7714.
[20] J. Li, D.B. Le, P.P. Ferguson, J.R. Dahn, Electrochim. Acta 55 (2010) 2991–2995.
[21] S. Komaba, T. Ozeki, N. Yabuuchi, K. Shimomura, Electrochemistry 79 (2011) 6–9.
[22] S. Komaba, K. Shimomura, N. Yabuuchi, T. Ozeki, H. Yui, K. Konno, J. Phys. Chem. C 115 (2011) 13487–13495.
[23] N. Yabuuchi, K. Shimomura, Y. Shimbe, T. Ozeki, J.Y. Son, H. Oji, Y. Katayama, T. Miura, S. Komaba, Adv. Energy Mater. 1 (2011) 759–765.
[24] A. Magasinski, B. Zdyrko, I. Kovalenko, B. Hertzberg, R. Burtovyy, C.F. Huebner, T.F. Fuller, I. Luzinov, G. Yushin, ACS Appl. Mater. Interfaces 2 (2010) 3004–3010.
[25] Z.J. Han, N. Yabuuchi, S. Hashimoto, T. Sasaki, S. Komaba, ECS Electrochem. Lett. 2 (2013) A17–A20.
[26] Z.J. Han, N. Yabuuchi, K. Shimomura, M. Murase, H. Yui, S. Komaba, Energy Environ. Sci. 5 (2012) 9014–9020.
[27] S. Komaba, T. Ozeki, K. Okushi, J. Power Sources 189 (2009) 197–203.
[28] S. Komaba, K. Okushi, T. Ozeki, H. Yui, Y. Katayama, T. Miura, T. Saito, H. Groult, Electrochem. Solid-State Lett. 12 (2009) A107–A110.
[29] S. Komaba, N. Yabuuchi, T. Ozeki, K. Okushi, H. Yui, K. Konnob, Y. Katayamac, T. Miurac, J. Power Sources 195 (2010) 6069–6074.
[30] K. Ui, S. Kikuchi, F. Mikami, Y. Kadoma, N. Kumagai, J. Power Sources 173 (2007) 518–521.
[31] K. Ui, J. Towada, S. Agatsuma, N. Kumagai, K. Yamamoto, H. Haruyama, K. Takeuchi, N. Koura, J. Power Sources 196 (2011) 3900–3905.
[32] Z.P. Cai, Y. Liang, W.S. Li, L.D. Xing, Y.H. Liao, J. Power Sources 189 (2009) 547–551.
[33] Z.A. Zhang, T. Zeng, C.M. Qu, H. Lu, M. Jia, Y.Q. Lai, J. Li, Electrochim. Acta 80 (2012) 440–444.
[34] Z.A. Zhang, T. Zeng, H. Lu, M. Jia, J. Li, Y.Q. Lai, ECS Electrochem. Lett. 1 (2012) A74–A76.
[35] Y. Liu, L. Tan, L. Li, J. Power Sources 221 (2013) 90–96.
[36] Y. Liu, L. Tan, L. Li, Chem. Commun. 48 (2012) 9858–9860.
[37] B. Koo, H. Kim, Y. Cho, K.T. Lee, N.S. Choi, J. Cho, Angew. Chem. Int. Ed. 51 (2012) 8762–8767.
[38] Y. Peng, P. Wu, Polymer 45 (2004) 5295–5299.
[39] P. Han, J. Fan, M. Jing, L. Zhu, X. Shen, T. Pan, J. Compos. Mater. 0 (2013) 1–8.
[40] S. Pejovnik, R. Dominko, M. Bele, M. Gaberscek, J. Jamnik, J. Power Sources 184 (2008) 593–597.
[41] B. Lestriez, C. R. Chim. 13 (2010) 1341–1350.